

Constraints on Core Collapse from the Black Hole Mass Function

C. S. Kochanek^{1,2}

¹ *Department of Astronomy, The Ohio State University, 140 West 18th Avenue, Columbus OH 43210*

² *Center for Cosmology and AstroParticle Physics, The Ohio State University, 191 W. Woodruff Avenue, Columbus OH 43210*

5 November 2021

ABSTRACT

We model the observed black hole mass function under the assumption that black hole formation is controlled by the compactness of the stellar core at the time of collapse. Low compactness stars are more likely to explode as supernovae and produce neutron stars, while high compactness stars are more likely to be failed supernovae that produce black holes with the mass of the helium core of the star. Using three sequences of stellar models and marginalizing over a model for the completeness of the black hole mass function, we find that the compactness $\xi_{2.5}$ above which 50% of core collapses produce black holes is $\xi_{2.5}^{50\%} = 0.24$ ($0.15 < \xi_{2.5}^{50\%} < 0.37$ at 90% confidence). While models with a sharp transition between successful and failed explosions are always the most likely ($\xi_{2.5}^{min} = \xi_{2.5}^{max}$), the width $\xi_{2.5}^{max} - \xi_{2.5}^{min}$ of the transition between the minimum compactness for black hole formation $\xi_{2.5}^{min}$ and the compactness $\xi_{2.5}^{max}$ above which all core collapses produce black holes is not well constrained. The models also predict that $f = 0.18$ ($0.09 < f < 0.39$) of core collapses fail assuming a minimum mass for core collapse of $8M_{\odot}$. We tested four other criteria for black hole formation based on $\xi_{2.0}$ and $\xi_{3.0}$, the compactnesses at enclosed masses of 2.0 or 3.0 rather than $2.5M_{\odot}$, the mass of the iron core, and the mass inside the oxygen burning shell. We found that $\xi_{2.0}$ works as well as $\xi_{2.5}$, while the compactness $\xi_{3.0}$ works significantly worse, as does using the iron core mass or the mass enclosed by the oxygen burning shell. As expected from the high compactness of 20–25 M_{\odot} stars, black hole formation in this mass range provides a natural explanation of the red supergiant problem.

Key words: stars: black holes – supernovae: general

1 INTRODUCTION

The mechanism of core collapse supernovae (ccSNe) remains an open problem despite over half a century of theoretical effort. In particular, theory cannot reliably predict which stars that undergo core collapse become ccSNe or which form black holes instead of neutron stars (e.g. Zhang et al. 2008, Nordhaus et al. 2010, O’Connor & Ott 2011, Fryer et al. 2012, Hanke et al. 2012, Takiwaki et al. 2012, Ugliano et al. 2012, Couch 2013, Dolence et al. 2013, Couch & O’Connor 2014, Dolence et al. 2014, Wong et al. 2014). Observationally, comparisons of massive star formation and SNe rates (Horiuchi et al. 2011, Botticella et al. 2012), limits on the diffuse SN neutrino background (Lien et al. 2010, Lunardini 2009), the Galactic rate (Adams et al. 2013), and direct searches for failed SNe (Kochanek et al. 2008, Gerke et al. 2014) limit the fraction of failed ccSNe to $f \lesssim 50\%$ of core collapses. There does, however, appear to be a deficit of higher mass ccSN progenitors (Kochanek et al. 2008), which is best quantified by the absence of red supergiant progen-

itors above $M \gtrsim 17M_{\odot}$ (Smartt et al. 2009). A natural explanation of this deficit is that $f \sim 20$ to 30% of core collapses fail to produce a ccSNe and instead form a black hole without a dramatic external explosion. Further progress in completing the mapping between progenitors and outcomes both for successful ccSNe and in searches for failed ccSNe should clarify these issues over the next decade.

We have few other probes of the ccSN mechanism other than this mapping between progenitors and external outcomes, although even this does not constrain the balance between neutron star and black hole formation in successful ccSNe. Neutrinos or gravity waves would be the best probe of the physics of core collapse, but this will only be possible for a Galactic supernova where the rates are low (once every ~ 50 years, Adams et al. 2013). Furthermore, the stellar mass function favors having a relatively low mass progenitor for which the neutrino mechanism for ccSNe works reasonably well and we have high confidence that the outcome is a neutron star (e.g., Thompson et al. 2003, Kitaura et al. 2006, Janka et al. 2008) rather than a rarer, higher mass

progenitor where the explosion mechanism and the type of remnant remains problematic. Even if the rate of failed cc-SNe is $f \simeq 20$ to 30%, the probability of detecting the formation of a black hole in the Galaxy is very low.

Another direct probe of the SN mechanism is the mass function of the remnant neutron stars and black holes (see, e.g., Bailyn et al. 1998, Özel et al. 2010, Farr et al. 2011, Kreidberg et al. 2012, Özel et al. 2012, Kiziltan et al. 2013). Most neutron star masses are clustered around $1.4M_{\odot}$, black hole masses are clustered around 5 to $10M_{\odot}$, and there is a gap (or at least a deep minimum) between the masses of neutron stars and black holes. Interpreting these results is challenging because these masses can only be measured in binaries and the selection functions for finding neutron star and black hole binaries are both different and difficult or impossible to model from first principles.

If, however, we assume that the separate mass distributions of neutron stars and black holes are relatively unbiased, then we can use them to constrain the physics of core collapse. For example, in Pejcha et al. (2012), we showed that the masses of double neutron star binaries strongly favored explosion models with no mass falling back onto the proto-neutron star and that the explosion probably develops at the edge of the iron core near a specific entropy of $S/N_A \simeq 2.8k_B$. Fall-back is traditionally invoked in order to explain how the observed masses of black holes can be less than the typical masses of their progenitors (e.g., Zhang et al. 2008, Fryer et al. 2012, Wong et al. 2014). However, in Kochanek (2014), we pointed out that failed ccSNe of red supergiants naturally produce black holes with the observed masses because the hydrogen envelope is ejected to leave a remnant that has the mass of the helium core (Nadezhin 1980, Lovegrove & Woosley 2013). Similarly, Burrows (1987) noted that stellar mass loss processes leads to stars (e.g., Wolf-Rayet stars) that will produce black holes with masses comparable to that of the helium core.

Based on these concepts, Clausen et al. (2014) associated the black hole mass with the helium core mass and then estimated the probability of black hole formation as a function of progenitor mass needed to explain the observed black hole mass function. As expected from the arguments in Kochanek (2014), this required a peak in the probability distribution at initial (ZAMS) masses of $M_0 = 20$ - $25M_{\odot}$ while also allowing a second peak at $M_0 \sim 60M_{\odot}$ because mass loss leads the Woosley & Heger (2007) progenitor models to produce the same helium core mass for two different initial masses. However, while stellar mass largely determines the fate of a star, it is not directly related to the physics of core collapse.

A more physical approach would be to relate the formation of a black hole to some property of the stellar core at the onset of collapse that is related to the likelihood of a successful explosion. This should not only lead to a more realistic model of the remnant mass distribution, but the parameter range needed to explain the mass function can then be used to inform models of core collapse. O’Connor & Ott (2011) argued that the compactness of the core defined by

$$\xi_M = \frac{M}{M_{\odot}} \frac{1000 \text{ km}}{R(M_{\text{bary}} = M)} \quad (1)$$

is a good metric for the “explodability” of a star. In particular, $\xi_{2.5}$, the compactness at a baryonic mass of $M_{\text{bary}} =$

$2.5M_{\odot}$, is a measure of how rapidly the density is dropping outside the iron core. If $\xi_{2.5}$ is small, the density is dropping rapidly and it is easier for neutrino heating or other physical effects to revive the shock and produce a successful explosion. The reverse holds if the compactness is high. Ugliano et al. (2012) argued for a lower compactness threshold than O’Connor & Ott (2011), and also considered the correlation of other properties of the core with the production of a successful explosion, finding relatively strong correlations with the binding energy of the material outside the iron core and little correlation with the mass of the iron core or the mass inside the oxygen burning shell. The compactness is not a simple function of progenitor mass, and Sukhbold & Woosley (2014) find that complex interactions between (in particular) carbon and oxygen burning shells can drive rapid variations in compactness with stellar mass.

In this paper, following the approach of Pejcha et al. (2012) for neutron stars, we model the observed black hole mass function to determine what explosion criteria will explain the black hole mass function under the assumption that the black hole mass equals the helium core mass at the time of explosion. While partly inspired by Clausen et al. (2014), our approach ties the model to the physics underlying the success of an explosion rather than the initial stellar mass. Unlike Clausen et al. (2014), we will also directly fit the data on black hole masses from Özel et al. (2010) rather than fitting their parametrized model of the black hole mass function. This is of some importance because the compactness is a complex function of initial mass, leading to a mass function with non-trivial structure. In §2 we summarize our statistical model, in §3 we present our results, and in §4 we discuss the future of this approach.

2 STATISTICAL METHODS

There are three elements to our calculation. First, we must estimate the probability $P(D_i|M_{BH})$ of the data D_i for black hole candidate system i given an estimated black hole mass M_{BH} . Second, we must estimate the probability $P_j(M_{BH}|\vec{p})$ of finding a black hole of mass M_{BH} given a set of model parameters \vec{p} describing the outcomes of core collapse for a set of models j . Third, we must have some set of priors $P(\vec{p})$ on the model parameters. Combining these terms using Bayes theorem, the probability distribution for our model parameters given the data on black holes is

$$P_j(\vec{p}|D) \propto P(\vec{p}) \Pi_i \int dM_{BH} P(D_i|M_{BH}) P_j(M_{BH}|\vec{p}). \quad (2)$$

If we only want to consider the probability distribution for the parameters of a particular model j , we simply normalize this distribution to unity. We can also compare different stellar models or criteria for black hole formation, where the probability of model j compared to all other models is

$$P_j(D) = \int d\vec{p} P_j(\vec{p}|D) \left[\sum_j \int d\vec{p} P_j(\vec{p}|D) \right]^{-1} \quad (3)$$

for models with the same numbers of parameters. This is basically the procedure that has been used extensively to estimate the intrinsic black hole mass distribution (Bailyn et al. 1998, Özel et al. 2010, Farr et al. 2011, Kreidberg et al.

2012, Özel et al. 2012, Kiziltan et al. 2013) but modified as done in Pejcha et al. (2012) to relate the data to an underlying model of core collapse rather than to a parametrized model of the remnant mass distribution.

For modeling the data, we simply follow the procedures and data summaries from Özel et al. (2010) with one exception. The probability $P(D_i|M_{BH})$ depends on the data available for each system. If both the mass ratio and inclination of a system are constrained, the probability distribution is described as a Gaussian

$$P(D_i|M_{BH}) \propto \exp[-(M_{BH} - M_i)^2/2\sigma_i^2] \quad (4)$$

where M_i and σ_i are the estimated mass and its uncertainty and the term is always normalized such that $\int P(D_i|M_{BH})dM_{BH} \equiv 1$. If the measured mass function is m_i with uncertainty σ_{mi} and the mass ratio q is restricted to the range $q_{min} < q < q_{max}$ then

$$P(D_i|M_{BH}) \propto \int_{q_{min}}^{q_{max}} dq \int_{x_m}^1 \frac{dx \exp[-(m_i - m)^2/2\sigma_{mi}^2]}{1 - x_m} \quad (5)$$

where $m = M_{BH} \sin^3 i / (1 + q)^2$, the inclination distribution is assumed to be uniform in $x = \cos i$ over $x_m < x < 1$, and the minimum inclination $x_m = 0.462(q/(1+q))^{1/3}$ is set by the requirement for having no eclipses. Finally, if there is also a constraint on the inclination, we include a multiplicative probability for the inclination, $\exp(-(i - i_0)^2/2\sigma_i^2)$. We could reproduce the results in Özel et al. (2010) if we also truncated the distributions at $M_{BH} = 50M_\odot$.

We model the probability of observing a black hole of mass M_{BH} as

$$P(M_{BH}|\vec{p}) \propto \sum_i \frac{dN}{dM_0} \left| \frac{dM_0}{dM_{BH}} \right|_i P(\xi(M_0))C(M_{BH}) \quad (6)$$

which is also normalized to unity, $\int P(M_{BH}|\vec{p})dM_{BH} \equiv 1$. The first term is a Salpeter progenitor mass function, $dN/dM_0 \propto M_0^{-2.35}$. The stellar models define a mapping $M_{BH}(M_0)$ between the initial mass and the helium core mass we use for the mass of the black hole. The second term comes from the variable transformation from M_0 in the progenitor mass function to M_{BH} in the black hole mass function. The effects of mass loss on higher mass stars means that the same black hole mass can result for two different progenitor masses, and we must sum over all solutions i .

The third term is the probability that a progenitor with some physical property $\xi(M_0)$ will form a black hole. This is a one-dimensional sequence of a variable like the compactness and we assume a simple model where $P(\xi) = 0$ for $\xi < \xi^{min}$, $P(\xi) = 1$ for $\xi > \xi^{max}$ and that $P(\xi)$ increases linearly over $\xi^{min} < \xi < \xi^{max}$. It is also useful to constrain $\xi^{50\%} = (\xi^{min} + \xi^{max})/2$, the value at which 50% of core collapses produce black holes. We might expect a sharp transition with $\xi^{min} = \xi^{max}$ at which stars either form black holes or not. However, there are many secondary variables (e.g., rotation, composition, binary mass transfer) that affect stellar evolution beyond mass, and stars of a given initial mass likely end with a distribution of compactnesses (or any other collapse criterion) at death. It is reasonable to assume this distribution is largely a spread in final compactnesses around the values for a particular sequence of progenitor models with mass, with the net effect of producing a smoothed $P(\xi)$ even if the true transition is sharp. Clausen et al. (2014)

proposed using a mass-dependent probability of black hole formation for similar physical reasons.

The final term, $C(M_{BH}) = (M_{BH}/10M_\odot)^\alpha$, models the completeness of the observed black hole mass function. Because $P(M_{BH}|\vec{p})$ is normalized to unit total probability (or, equivalently, that we have no constraint on the absolute number of black holes), only the shape and not the normalization of $C(M_{BH})$ affects the results. If $\alpha > 0$ we are more likely to find high mass black holes, and the reverse if $\alpha < 0$. Completeness and biases have always been a significant concern for interpreting the black hole mass function, particularly because black hole masses are only measured in interacting binaries (see, Bailyn et al. 1998, Özel et al. 2010, Farr et al. 2011, Kreidberg et al. 2012, Özel et al. 2012, Clausen et al. 2014). Whatever biases exist, they are probably a relatively smooth function of mass and including $C(M_{BH})$ allows us to test for their effects or to simply marginalize over α as a nuisance parameter.

Our model parameters, such as the compactness limits or the exponent of the completeness function, all have limited dynamic ranges making uniform priors a reasonable choice. For comparisons between models with different parameters (Equation 3), we normalize the priors as $\int P(\vec{p})d\vec{p} \equiv 1$ over the range used for the calculation. This will give different models equal relative probabilities in Equation 3 unless the data significantly discriminates between the models.

We also compute the fraction f of core collapses leading to black holes under the assumption that all stars with $M_0 > 8M_\odot$ undergo core collapse. We include a weak prior $P(f)$ on the models using the constraints derived by Adams et al. (2013) from combining the observed Galactic SN rate with the lack of any neutrino detection of a Galactic black hole formation event. A stiffer limit of $f < 0.5$ could probably be justified based on comparisons of SN and star formation rates (Horiuchi et al. 2011) or limits on the diffuse neutrino background (Lien et al. 2010), but these introduce a dependence on estimates of star formation rates and are difficult to translate into a mathematical prior. These estimates of f are contingent on the normalization that $P(\xi(M_0))$ becomes unity for $\xi > \xi^{max}$. We could allow $P(\xi(M_0)) = P_{max} < 1$ for $\xi > \xi^{max}$ without any consequences for our models of the black hole mass function, and this would reduce f .

While there are differences in the details of the analyses by Özel et al. (2010), Farr et al. (2011) and Özel et al. (2012), the primary differences in the results are driven by differences in the samples of black hole candidates. Özel et al. (2010) and Özel et al. (2012) analyze a sample of 16 systems with low mass companions, while Farr et al. (2011) analyze 15 low mass systems, where GC 339–4 is the system that is not in common. For these low mass systems, the resulting inferences about the black hole mass functions are mutually consistent. Farr et al. (2011) also carries out the analysis including 5 systems with high mass companions. These systems generally have probability distributions requiring significantly higher masses than the low mass sample, and the inferred black hole mass functions have significantly more probability for $M_{BH} > 10M_\odot$ with their inclusion.

Like the question of differences in selection functions for neutron stars and black holes, the relative selection functions

for black hole systems with high and low mass companions probably cannot be derived. However, the sharply declining mass functions found from using only the low mass systems are hard to reconcile with the existence of the high mass systems. For example, for an exponential mass function, $dN/dM_{BH} \propto \exp(-M_{BH}/M_s)$ with $M_c < M_{BH} < 50M_\odot$ fit to the low mass samples, Özel et al. (2012) finds $M_c = 6.32M_\odot$ and $M_s = 1.61M_\odot$ while Farr et al. (2011) finds $M_c = 6.03M_\odot$ and $M_s = 1.55M_\odot$. These low mass samples exclude the high mass system Cyg X1, which has an improved mass estimate of $M_{BH} = (14.8 \pm 1.0)M_\odot$ by Orosz et al. (2011) (although Ziółkowski 2014 argues the uncertainties are somewhat larger). Given the sample sizes, the probability of finding a system as massive as Cyg X1 based on these mass functions is only about 5%. Clearly, adding the information that these generally higher black hole mass, high companion mass systems exist will change the inferences from the low mass systems, just as found by Farr et al. (2011).

However, of the five high mass systems included by Farr et al. (2011), only Cyg X1 is a Galactic source. If, as seems likely given the existing samples, the high mass X-ray binaries tend to host higher mass black holes than the low mass X-ray binaries, then including the four extragalactic high mass systems without their accompanying low mass companions could be biasing the estimates of the mass function in the other direction. As an imperfect compromise, we model the 16 low mass systems following Özel et al. (2010) and include Cyg X1 with a Gaussian probability distribution of mean $14.8M_\odot$ and dispersion $2.0M_\odot$ (Equation 4), doubling the uncertainties from Orosz et al. (2011) based on the arguments in Ziółkowski (2014). This gives us a sample of 17 mass estimates.

In order to compare to the earlier studies, we fit the data using both an exponential and a power-law ($dN/dM_{BH} \propto \exp(-M_{BH}/M_s)$ or $\propto M_{BH}^\beta$ for $M_c < M_{BH} < 50M_\odot$) parametric mass function. For these calculations, Equation 6 is simply replaced by the appropriate parametric form. We used uniform priors for the two parameters in each model. Figure 1 shows the results for the exponential mass function, where we find a median cutoff mass of $M_c = 5.98M_\odot$ ($4.94M_\odot < M_c < 6.51M_\odot$) and an exponential scale mass of $M_s = 2.99M_\odot$ ($1.55M_\odot < M_s < 5.85M_\odot$) where we always present 90% confidence intervals. As expected from adding Cyg X1, we find an exponential scale mass that is larger than the results from Özel et al. (2010), Farr et al. (2011) and Özel et al. (2012) using only the low companion mass sample, but smaller than the results from Farr et al. (2011) including all the high companion mass systems. For the power law model we find $M_c = 6.21M_\odot$ ($5.57M_\odot < M_c < 6.62M_\odot$) and $\beta = -4.87$ ($-7.93 < \beta < -3.00$). Unlike Farr et al. (2011), we used a fixed upper mass cutoff at $M_{BH} = 50M_\odot$, but the Farr et al. (2011) estimates of $M_c = 6.10M_\odot$ ($1.28M_\odot < M_c < 6.63M_\odot$ with $\beta = -6.39$ ($-12.42 < \beta < 5.69$) for their low mass sample and $M_c = 5.85M_\odot$ ($4.87M_\odot < M_c < 6.46M_\odot$) with $\beta = -3.23$ ($-5.05 < \beta < -1.77$) for their combined sample appear compatible with our estimates. The relative probabilities of these two models are about 1.4 in favor of the exponential model, but this is well within the regime where the results will be dominated by the effects of priors (through

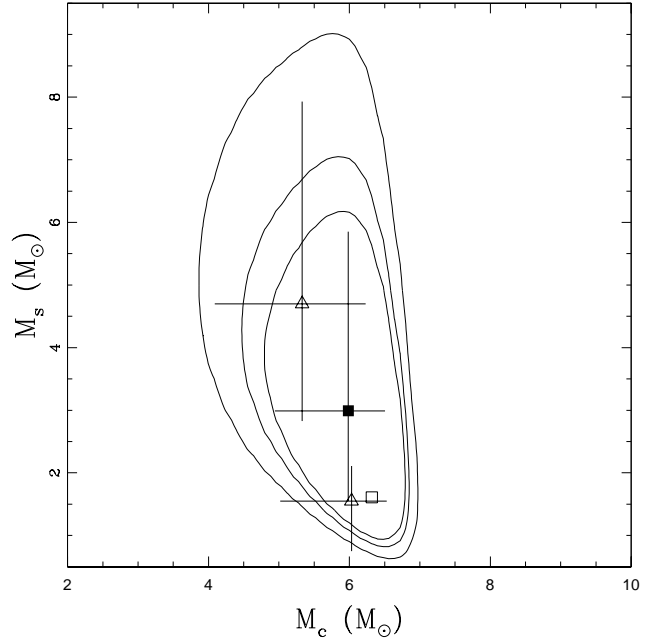


Figure 1. Probability contours for the exponential parametric model, $dN/M_{BH} \propto \exp(-M/M_s)$ for $M_c < M_{BH} < 50M_\odot$, of the black hole mass function. The probability contours enclose 90%, 95% and 99% of the probability computed over the parameter range shown. The filled square with error bars shows the median value and the 90% confidence range for each parameter. The open square with no error bar shows the result from Özel et al. (2012) using only low mass systems. The open triangles with error bars show the results from Farr et al. (2011) for only low mass systems (lower) or both low and high mass systems (upper). Our addition of one high mass system, Cyg X1, to the Özel et al. (2010) sample produces an intermediate result.

the choice of the parameter range over which we carried out the probability integrals).

3 RESULTS

We consider the Woosley et al. (2002) and Woosley & Heger (2007) Solar metallicity progenitor models. The Woosley et al. (2002) models span $10.8M_\odot < M_0 < 70M_\odot$ with a relatively dense sampling ($\Delta M = 0.2M_\odot$) from $10.8M_\odot$ to $30M_\odot$, a coarser sampling ($\Delta M = 1.0M_\odot$) to $40M_\odot$ and then a last model at $75M_\odot$. The Woosley & Heger (2007) models span $12M_\odot < M_0 < 120M_\odot$ sampling every $\Delta M = 1.0M_\odot$ up to $35M_\odot$, every $\Delta M = 5.0M_\odot$ to $60M_\odot$, and models at 70, 80, 100 and $120M_\odot$. Sukhbold & Woosley (2014) supplemented the Woosley & Heger (2007) models, sampling the range from 15 to $30M_\odot$ with $\Delta M = 0.1M_\odot$. We assume models from $8M_\odot$ to $75M_\odot$ for the Woosley et al. (2002) models or $120M_\odot$ for the Woosley & Heger (2007) models undergo core collapse and allow black hole formation only over the mass range of the model sequences. Stars with masses from $8M_\odot$ to the minimum masses of the sequences (10.8 or $12M_\odot$) are assumed to be successful SNe forming neutron stars. We will refer to the three progenitor sequences as the W02, W07, and W07+S14 models.

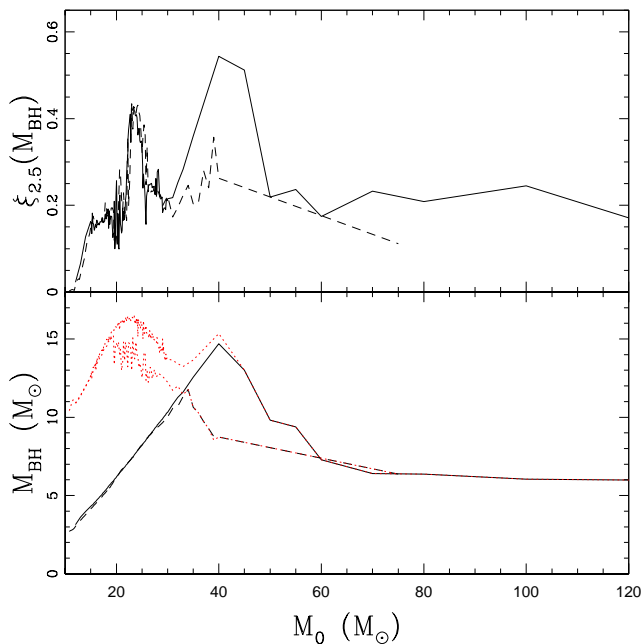


Figure 2. Compactness $\xi_{2.5}$ (top) and black hole mass (bottom) as a function of the initial stellar mass. The solid lines are for the Woosley & Heger (2007) and Sukhbold & Woosley (2014) models while the dashed lines are for the Woosley et al. (2002) models. In the lower panel, dotted red lines show the final masses of the star. The hydrogen mass at death (the mass difference between the total mass and the helium core/black hole mass) is assumed to be ejected by the Nadezhin (1980) mechanism in a failed supernova.

For each model we computed the mass of the helium core, defined by the radius where $X_H = 0.2$, and the compactness ξ_M (Equation 1) for $M_{\text{barry}} = 2.0, 2.5$ and 3.0 based on the progenitor model. For the densely sampled mass ranges we slightly smoothed the helium core masses as a function of mass to remove small fluctuations that complicate the mapping from initial mass into black hole mass due to the derivative in Equation 6. Following Ugliano et al. (2012) we also computed the mass of the iron core (M_{Fe} , defined by the point where $Y_e = 0.497$) and the mass at the inner edge of the oxygen burning shell (M_O , defined by the point where the dimensionless entropy per baryon equaled 4) for the W02 and W07 models. We did not possess the density profiles needed to compute these properties for the S14 models, but Sukhbold & Woosley (2014) kindly supplied a table of their helium core masses and $\xi_{2.5}$.

O’Connor & Ott (2011) argue that $\xi_{2.5}$ should be computed at the time of core bounce, while Sukhbold & Woosley (2014) note that computing it when the collapse speed reaches 1000 km/s produces equivalent results and Ugliano et al. (2012) note that there is little difference between simply calculating it from the progenitor model and calculating it at the time of core bounce. Operationally, simply using the compactness of the progenitor is far simpler because it avoids simulating a portion of the collapse for each model. If we use the O’Connor & Ott (2011) or Sukhbold & Woosley (2014) values, we find no significant differences from our results simply using the values estimated from the progenitors.

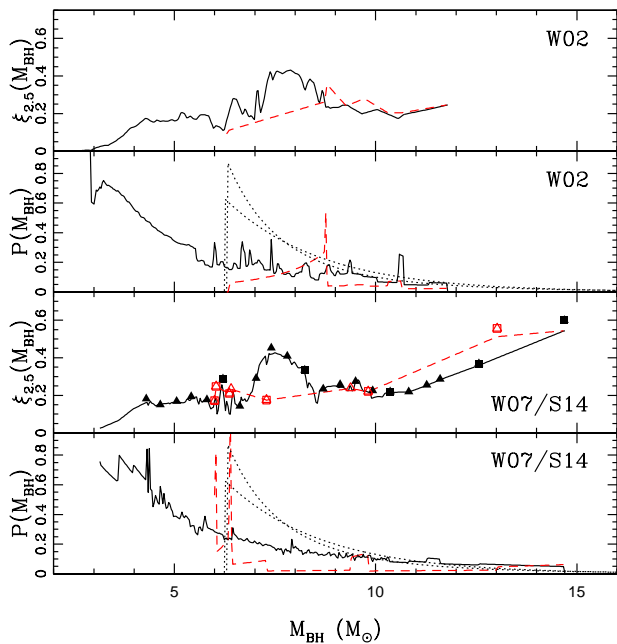


Figure 3. Compactness $\xi_{2.5}$ as a function of black hole mass and the black hole mass function if all stars formed black holes with the masses of their helium cores for the W02 (top two panels) and W07+S14 (bottom two panels) models. The solid black (dashed red) lines show the contributions from progenitors below (above) the stellar mass producing the peak helium core mass. The normalizations of the mass functions are arbitrary. The squares and triangles in the compactness panel for the W07+S14 models show the compactness estimates for the same cases from O’Connor & Ott (2011) and Sukhbold & Woosley (2014), respectively. Filled black (open red) symbols correspond to low (high) mass progenitors. As noted by Ugliano et al. (2012) there is little difference between the compactness estimates. The mass function panels include the parametric mass functions with the median parameter estimates from §2 as the dotted curves.

Figure 2 shows the helium core mass, which we now define to be the black hole mass, and the compactness $\xi_{2.5}$ as a function of the initial stellar mass M_0 . The main qualitative difference is that the Woosley et al. (2002) models have a lower maximum helium core mass and a significantly smaller and lower compactness peak near $M_0 \simeq 40M_{\odot}$. The other compactness sequences look similar but with modest changes in the average level and the ratio of the peaks near 20-25 and $40M_{\odot}$.

Figure 2 also shows the total mass when the star explodes, and we assume that any remaining hydrogen envelope is ejected. For a failed supernova of a red supergiant, which represents the bulk of any models with residual hydrogen, the Nadezhin (1980) mechanism naturally does so, as seen in the simulations of Lovegrove & Woosley (2013). For the higher mass stars, mass loss has stripped the hydrogen prior to the explosion. As the amount of residual hydrogen becomes negligible, the stellar envelope will collapse and the Nadezhin (1980) mechanism cannot work because it depends on the very low binding energy of a red supergiant envelope. At this point, however, the correction from adding the remaining hydrogen to the black hole is also unimportant. While we are phrasing black hole formation as being

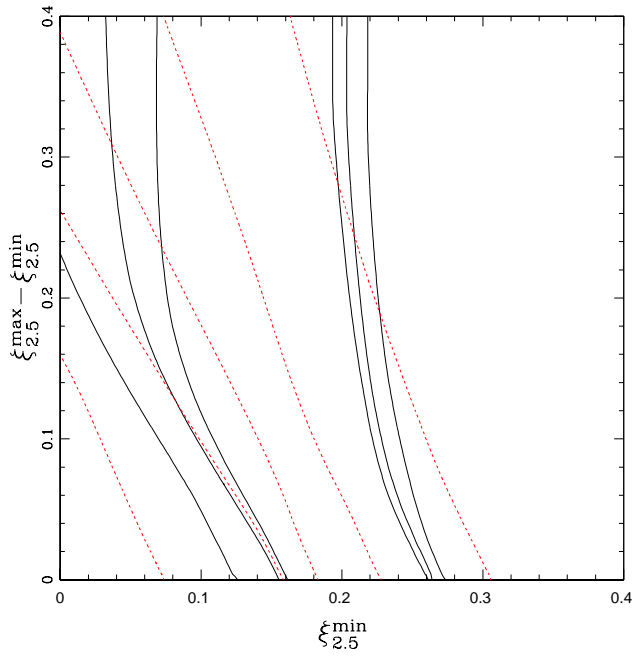


Figure 4. Constraints on the compactness $\xi_{2.5}$ for the W07 model assuming no biases in the black hole mass function ($\alpha = 0$). The probability contours enclose 90, 95 and 99% of the total probability for a uniform prior over the region shown. The red dotted lines show contours of the failed ccSNe fraction with $f = 0.1, 0.2, 0.3, 0.4$ and 0.5 (from right to left).

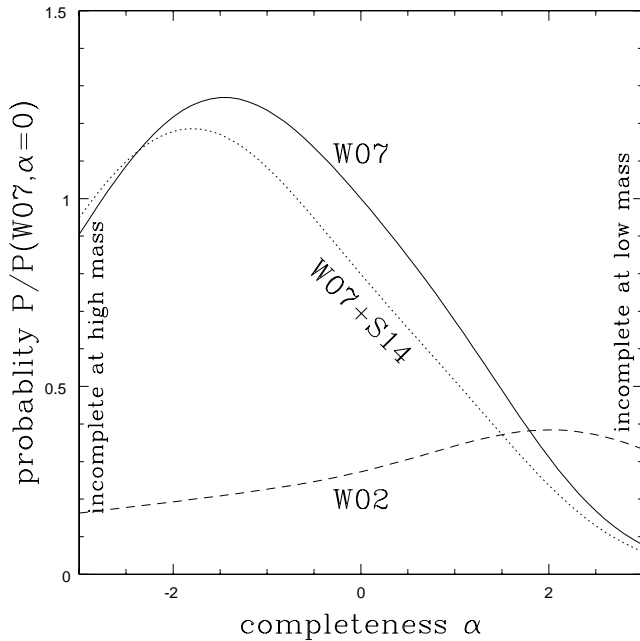


Figure 5. Model probabilities as a function of the completeness exponent α for the W02 (dashed), W07 (solid) and W07+S14 (dotted) $\xi_{2.5}$ models. The probabilities are relative to the $\alpha = 0$ W07 model. The mass function is incomplete at high mass for $\alpha < 0$ and incomplete at low mass for $\alpha > 0$.

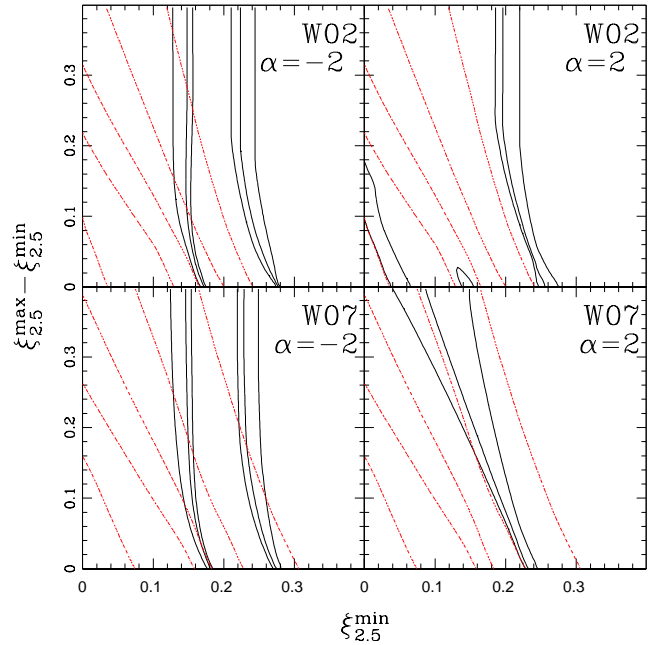


Figure 6. Constraints on the compactness $\xi_{2.5}$ as a function of the completeness. The top panels are for the W02 model and the bottom panels are for the W07 model. The left panels assume the observations are more complete for low mass black holes ($\alpha = -2$) while the right panels assume the observations are more complete for high mass black holes ($\alpha = 2$). Low values of $\xi_{2.5}^{min}$ are favored in the $\alpha = 2$ models. The probability contours enclose 90, 95 and 99% of the total probability for each model. The red dotted lines show contours of the failed ccSNe fraction with $f = 0.1, 0.2, 0.3, 0.4$ and 0.5 (from right to left).

due to failed SNe, fine tuning fall back could produce the same black hole masses in successful SNe.

Figure 3 shows the structure of these models as a function of black hole mass. Because the black hole mass peaks at an intermediate initial mass, there are two branches to the solutions, corresponding to initial masses above and below this maximum. Broadly speaking, there is an extended plateau in $\xi_{2.5}$ starting near $M_{BH} \simeq 4M_{\odot}$ with a rapid drop at lower masses, a narrow peak near $6M_{\odot}$ and a broader peak near $8M_{\odot}$. We also show the $\xi_{2.5}$ values from O’Connor & Ott (2011) and Sukhbold & Woosley (2014), and we see that there are few differences from our estimates simply using the structure of the progenitor, as previously noted by Ugliano et al. (2012).

We also show the black hole mass functions which would result from all the models becoming black holes with the mass of the helium core. The general decline of the Salpeter mass function is visible, but the slope of $M_{BH}(M_0)$ introduces significant structure. The broader trends are real features of the models, but some of the small scale structure is due to “noise” in $M_{BH}(M_0)$. Whenever $M_{BH}(M_0)$ is locally flat, the derivative term in Equation 6 leads to a local peak in the mass function. The smoothing we used to make the $M_{BH}(M_0)$ profiles monotonic outside of the single peak significantly reduces these features compared to the raw relations. None of these local structures are important because they are changes in the mass function on such small scales

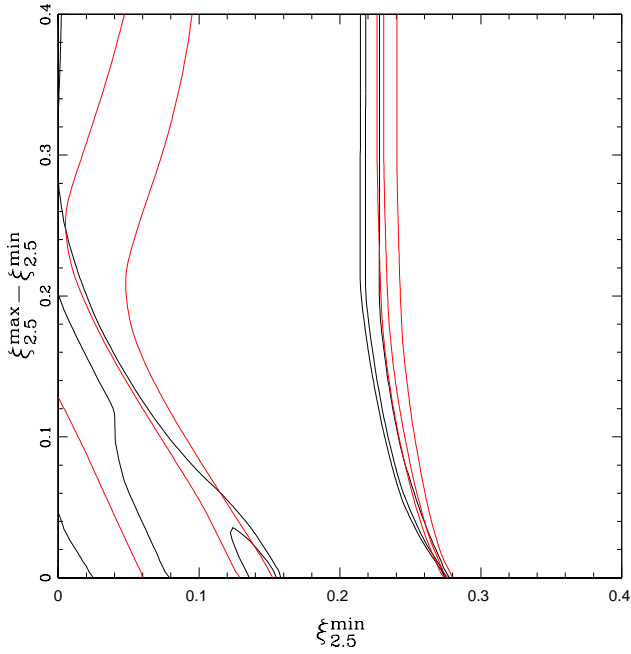


Figure 7. Constraints on the compactness $\xi_{2.5}$ marginalized over completeness ($-3 < \alpha < 3$) for the W02 (black solid) and W07 (red dotted) models. The results for the W07+S14 models are very close to those for the W07 models. The probability contours enclose 90, 95 and 99% of the total probability for each model.

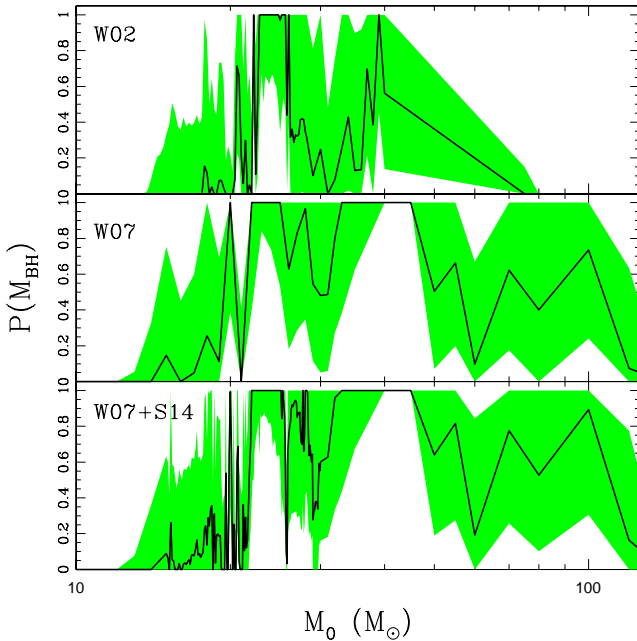


Figure 8. Probability of black hole formation as a function of initial stellar mass for $\alpha = 0$ and the W02 (top), W07 (middle) and W07+S14 (bottom) models after marginalizing over $\xi_{2.5}^{\min}$ and $\xi_{2.5}^{\max}$. The heavy black line is the median probability and the shaded band is the 90% confidence range. The estimates are highly correlated between different masses.

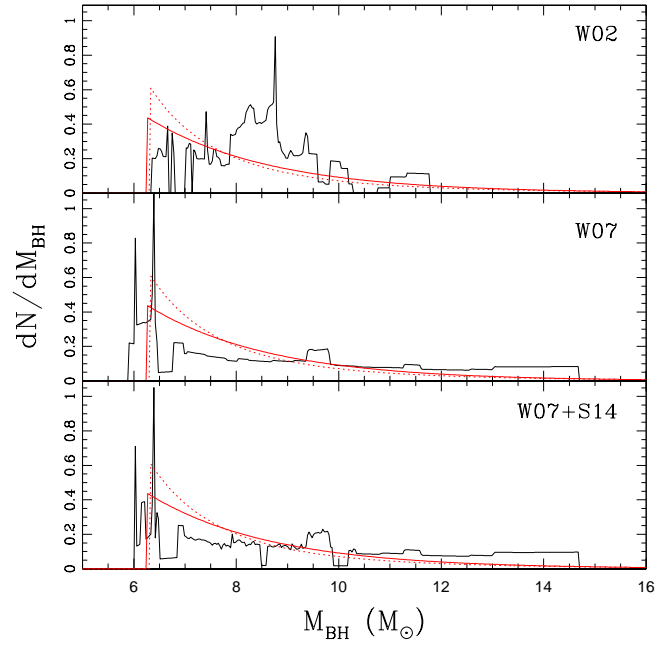


Figure 9. Maximum likelihood mass functions for the W02 (top), W07 (middle) and W07+S14 models with $\alpha = 0$. They are normalized to have the same integrated area. For comparison, the red solid and dashed curves show the parametric mass function estimates from §2. Most of the structures here are real and are created by the rapid changes of the compactness with M_0 in some mass ranges (see Sukhbold & Woosley 2014).

that they have no consequences for modeling the data. For comparison, we also show the two parametric estimates of the black hole mass function from §2. Producing a similar mass function requires suppressing the formation of low mass black holes. The mass functions derived from the stellar models do not decline as rapidly as the parametric models, which could be a problem in either of the models or a consequence of completeness in the black hole sample.

We first consider the three models using $\xi_{2.5}$ and no mass-dependent completeness effects ($\alpha = 0$). These W02, W07 and W07+S14 models have probabilities relative to the exponential parametric model of 0.7, 2.5 and 2.0, respectively. Thus, our first result is that our models based on progenitor models and a physical criterion for black hole formation can fit the observed mass function just as well as standard parametric models. However, given the changing parameters and parameter ranges, the differences are not large enough to argue that the $\alpha = 0$ W07 model is significantly better. Between the three stellar models, the ratios are 0.27 : 1.0 : 0.80, favoring the W07 model but not by a large enough factor to rule out the W02 model. This ordering is driven by the inclusion of Cyg X1. If we drop it, the relative probabilities are 1 : 0.33 : 0.26 and the W02 model is favored over the W07 model. These shifts are driven by the relative areas of the compactness peaks in the two models: with Cyg X1, W02 produces too few massive black holes, and without Cyg X1, W07 produces too many. We will explore this in more detail when we discuss the effects of the completeness model.

Figure 4 shows the likelihood function for the $\alpha = 0$, $\xi_{2.5}$

W07 model as well as the fractions of core collapses becoming black holes. The structures of the W02 and W07+S14 results are similar. The compactness threshold $\xi_{2.5}^{min}$ for black hole formation is well constrained. Although the most probable model is always for a sharp transition with $\xi_{2.5}^{max} = \xi_{2.5}^{min}$, the width of the transition, $\xi_{2.5}^{max} - \xi_{2.5}^{min}$, is not well constrained. Formally, the median estimates are $\xi_{2.5}^{min} = 0.17$ ($0.07 < \xi_{2.5}^{min} < 0.23$), $\xi_{2.5}^{min} = 0.16$ ($0.06 < \xi_{2.5}^{min} < 0.22$), and $\xi_{2.5}^{min} = 0.15$ ($0.06 < \xi_{2.5}^{min} < 0.20$) for the W02, W07 and W07+S14 models, respectively. This is somewhat misleading because the lower values of $\xi_{2.5}^{min}$ are associated with wide transitions. A better metric is probably $\xi_{2.5}^{50\%} = (\xi_{2.5}^{min} + \xi_{2.5}^{max})$, the point where the probability of forming a black hole becomes 50%. For these models we find that $\xi_{2.5}^{50\%} = 0.24$ ($0.17 < \xi_{2.5}^{50\%} < 0.36$), $\xi_{2.5}^{50\%} = 0.23$ ($0.17 < \xi_{2.5}^{50\%} < 0.33$), and $\xi_{2.5}^{50\%} = 0.21$ ($0.16 < \xi_{2.5}^{50\%} < 0.32$), so $\xi_{2.5}^{50\%}$ is constrained to be close the plateau in $\xi_{2.5}$ seen in Figure 3 and high enough to largely prevent black hole formation at lower masses where the compactness is dropping rapidly. As we will see, this is sufficient to lead to a sharp break in the black hole mass function just as is included in the parametric models. These estimates from fitting the observed black hole mass function are quite similar to the range of 0.15 to 0.35 found by Ugliano et al. (2012) in their core collapse simulations and lower than the limit proposed by O’Connor & Ott (2011). The fractions of core collapses producing black holes are $f = 0.13$ ($0.05 < f < 0.28$), $f = 0.21$ ($0.11 < f < 0.34$), and $f = 0.21$ ($0.11 < f < 0.33$), respectively, where the W07 models produce larger numbers of black holes because of the prominent compactness peak near $M_0 = 40M_\odot$. If we arbitrarily remove this peak by setting $\xi_{2.5} = 0.2$ in this regime, the results more closely resemble those for the W02 models.

For the W02 and W07 models we can also examine using the compactness at another mass cut, $\xi_{2.0}$ or $\xi_{3.0}$, the iron core mass, M_{Fe} , or the mass at inner edge of the oxygen burning shell, M_O , as the criterion for forming a black hole. The procedure is the same in each case, we raise the probability for forming a black hole linearly from zero at one value of the parameter to unity at a higher value. For the $\alpha = 0$ W02 models, the relative probabilities of the criteria are 1.97 : 1.00 : 0.31 : 0.19 : 0.20 for $\xi_{2.0}$, $\xi_{2.5}$, $\xi_{3.0}$, M_{Fe} and M_O , respectively, where we have normalized the models to the standard $\xi_{2.5}$ model. For the $\alpha = 0$ W07 models, the ratios are 1.11 : 1.00 : 0.52 : 0.28 : 0.03. This general structure holds when we vary the completeness as well. If we simply marginalize over the completeness ($-3 < \alpha < 3$ with a uniform prior) and the W02 and W07 models, the probabilities of the formation criteria relative to the $\xi_{2.5}$ model are 0.92 : 1.00 : 0.39 : 0.29 : 0.14. The compactness at a smaller mass cut $\xi_{2.0}$ is almost equally good, the compactness at a larger mass cut $\xi_{3.0}$ is moderately worse, the iron core mass is an even poorer model, and the oxygen burning shell mass is the worst model. Arguably, only M_O shows a large enough probability ratio to be rejected at a reasonable confidence level. These results are consistent with the simulations of Ugliano et al. (2012), who found that M_{Fe} and M_O had poorer correlations with black hole formation than $\xi_{2.5}$. For the remainder of the paper we will just consider the $\xi_{2.5}$ model.

Figure 5 shows the relative probabilities of the W02, W07 and W07+S14 $\xi_{2.5}$ models as a function of the com-

pleteness exponent α . The W02 models modestly prefer incompleteness at low mass, while the W07 and W07+S14 models more strongly prefer incompleteness at high mass. We only explored the range $-3 < \alpha < 3$ with a uniform prior. All three cases peak in this range and larger values of $|\alpha|$ seemed unreasonable – for $|\alpha| = 3$, the relative completeness changes by a factor of 8 between $M_{BH} = 5$ and $10M_\odot$. The qualitative differences can be understood from the differences in the $\xi_{2.5}$ profiles shown in Figures 2 and 3. The peak near $M_0 = 40M_\odot$ which produces the most massive black holes is weaker compared to the peak near $M_0 = 20$ – $25M_\odot$ in the W02 models relative to the W07 or W07+S14 models. Compared to the data, the W02 model produces too few high mass black holes and so to compensate the models make the observed sample incomplete at low masses. The W07 models produce too many high mass black holes, and compensate by making the observed sample incomplete at high mass. If we exclude Cyg X1, then all three models favor observational samples that are incomplete at high black hole mass.

The completeness probability distributions are related to the results of Clausen et al. (2014) in their estimate of the probability of black hole formation as a function of initial stellar mass M_0 . Their formation probability distribution has a peak associated with the first peak in $\xi_{2.5}$ at $M_0 = 20$ – $25M_\odot$ but no peak associated with the second peak in $\xi_{2.5}$ near $M_0 = 40M_\odot$. They derived the probability distributions by fitting the parametric mass functions of Özel et al. (2012), which are based on only the low mass binaries and have low probabilities for higher mass black holes. The lack of a probability peak near $M_0 = 40M_\odot$ is similar to the effects of $\alpha < 0$.

For comparison to the mass-independent completeness case in Figure 4, Figure 6 shows the results for the W02 and W07 models with $\alpha = -2$ and 2. This corresponds to changing the completeness between $M_{BH} = 5M_\odot$ and $10M_\odot$ by a factor of 4. When the discovery of low mass black holes is favored ($\alpha = -2$), the upper limits on $\xi_{2.5}^{min}$ change little but the lower limits become much stronger. When the discovery of high mass black holes is favored ($\alpha = 2$), the upper limit on $\xi_{2.5}^{min}$ becomes somewhat stronger, while the lower limit becomes significantly weaker. As the completeness for low mass black holes decreases, there is more freedom to make them. This can be seen in the fractions of core collapses producing black holes, which are $f = 0.10$ ($0.04 < f < 0.20$) and 0.08 ($0.14 < f < 0.25$) for the W02 and W07 models with $\alpha = -2$ but $f = 0.20$ ($0.06 < f < 0.45$) and $f = 0.34$ ($0.18 < f < 0.51$) for the $\alpha = 2$ models.

Finally, we can also marginalize over the completeness model ($-3 < \alpha < 3$ with a uniform prior). Marginalized over α , the relative probabilities of the W02, W07 and W07+S14 $\xi_{2.5}$ models are 0.33 : 1.00 : 0.88, moderately favoring the W07 models. Figure 7 shows the constraints on the compactness parameters for the W02 and W07 models marginalized over completeness. The hard upper limit is robust, but the lower limit becomes soft because of the contribution from the $\alpha > 0$ models. The estimates of the critical compactness $\xi_{2.5}^{min}$ are $\xi_{2.5}^{min} = 0.17$ ($0.03 < \xi_{2.5}^{min} < 0.23$), $\xi_{2.5}^{min} = 0.18$ ($0.05 < \xi_{2.5}^{min} < 0.23$), and $\xi_{2.5}^{min} = 0.17$ ($0.05 < \xi_{2.5}^{min} < 0.21$) for the W02, W07 and W07+S14 models, respectively. The constraints on $\xi_{2.5}^{50\%}$, the compactness where the probability of forming a black hole is 50%, are tighter, with $\xi_{2.5}^{50\%} = 0.23$

($0.11 < \xi_{2.5}^{50\%} < 0.35$), $\xi_{2.5}^{50\%} = 0.24$ ($0.15 < \xi_{2.5}^{50\%} < 0.37$), and $\xi_{2.5}^{50\%} = 0.23$ ($0.14 < \xi_{2.5}^{50\%} < 0.35$). Finally, the constraints on the fraction of core collapses leading to black holes are $f = 0.14$ ($0.05 < f < 0.41$), $f = 0.18$ ($0.09 < f < 0.39$), and $f = 0.18$ ($0.09 < f < 0.38$). Despite allowing for very large, black hole mass-dependent completeness corrections, the constraints on $\xi_{2.5}^{50\%}$ and f are quite strong.

Clausen et al. (2014) estimated the probability of forming a black hole with the mass of the helium core as a function of initial stellar mass needed to match the Özel et al. (2012) parametric model of the black hole mass function. For a given model, we can marginalize over $\xi_{2.5}^{min}$ and $\xi_{2.5}^{max}$ to estimate this probability as a function of mass as well as its variance over the model space, although the uncertainty estimates are highly correlated. The results for the $\alpha = 0$ case are shown in Figure 8. Black hole formation is disfavored below $M_0 \simeq 20M_\odot$ with the probability steadily dropping towards lower masses. Black hole formation is probably required near $20\text{--}25M_\odot$ and near $40M_\odot$. At most other masses, the data do not strongly constrain the probability of forming a black hole.

Finally, in Figure 9 we show the maximum likelihood mass functions for the three $\alpha = 0$, $\xi_{2.5}$ models as compared to the median fit parametric exponential and power-law models from §2. Our models roughly match the minimum black hole masses of the parametric models. The W07 and W07+S14 mass functions are relatively flat due to the broad compactness peak at $M_0 \sim 40M_\odot$, while the W02 mass function is more strongly peaked at low masses. The absence of higher mass black holes in the W02 models as compared to the W07/W07+S14 models explains why the W07/W07+S14 models are favored with the inclusion of Cyg X1.

4 DISCUSSION

If black hole formation is controlled by the compactness of the stellar core at the time of collapse (e.g., O’Connor & Ott 2011, Ugliano et al. 2012, Sukhbold & Woosley 2014) and we associate the mass of the resulting black hole with the mass of the helium core (e.g., Burrows 1987, Kochanek 2014, Clausen et al. 2014) then we can constrain the compactness above which black holes form by fitting the observed black hole mass function (e.g., Bailyn et al. 1998, Özel et al. 2010, Farr et al. 2011, Kreidberg et al. 2012, Özel et al. 2012). The helium core mass is a natural scale for black hole masses due to either mass loss (e.g., Burrows 1987) or the physics of failed ccSNe (Nadezhin 1980, Lovegrove & Woosley 2013, Kochanek 2014). We also, for the first time, include a model for the completeness of the observed sample of black holes and examine its consequences for the constraints on the core collapse parameters.

We use a sample of 17 black hole candidates, the 16 low mass binary systems used by Özel et al. (2010) and Özel et al. (2012) combined with the one Galactic high mass system, Cyg X1. Farr et al. (2011) found that the parameters of their models of the black hole mass function changed significantly when the high mass binaries were included in the analysis because they tend to have higher average masses. Including Cyg X1 is a compromise between excluding all high mass systems (Özel et al. 2010, Özel et al.

2012, Farr et al. 2011) and including all high mass systems (Farr et al. 2011). We exclude the extragalactic high mass systems since there is no equivalent sample of extragalactic low mass systems. Where necessary, we discuss the impact of including Cyg X1 on the results. If we model the data using the parametric methods and models of these previous studies, we obtain similar results.

The first interesting result is that our models based on combining progenitor models with a physical criterion for forming a black hole fit the observed black hole mass function as well as the existing parametric models. Our best model actually has a higher likelihood, but the likelihood ratios are not large enough to be significant. Unlike the simple parametric models, the mass functions produced by our models have a great deal of structure (Figure 9) created by the rapid variations in compactness with mass (Figures 2 and 3).

We tested five different parameters for predicting the formation of a black hole. The compactnesses $\xi_{2.0}$, $\xi_{2.5}$ and $\xi_{3.0}$ of the core of the progenitor at baryonic masses of 2.0, 2.5 and $3.0M_\odot$ (Equation 1), the mass of the iron core M_{Fe} and the mass inside the oxygen burning shell M_O . We considered three sets of stellar models, W02 from Woosley et al. (2002), W07 from Woosley & Heger (2007), and W07+S14 which supplements the W07 models with the denser mass sampling from Sukhbold & Woosley (2014). Marginalizing over all our other variables, we find that the compactnesses $\xi_{2.0}$ and $\xi_{2.5}$ produced the highest likelihoods. The compactness $\xi_{3.0}$ models were somewhat less probable, the iron core mass models still less so, and the oxygen shell mass models were the worst. With overall likelihood ratios relative to the $\xi_{2.5}$ model of 0.92 : 1.00 : 0.39 : 0.29 : 0.14 none of the other possibilities are strongly ruled out. Ugliano et al. (2012) found in their simulations that the compactness was a better predictor of outcomes than the iron core or oxygen shell masses. We now focus on the $\xi_{2.5}$ models.

The relative probabilities of the W02, W07 and W07+S14 $\xi_{2.5}$ models after marginalizing over the completeness model are 0.33 : 1.00 : 0.88, favoring the W07 models. The origin of the differences are due to the relative strengths of the peaks in the compactness as a function of mass near $M_0 = 20\text{--}25M_\odot$ and $M_0 = 40M_\odot$, which control the relative production of higher and lower mass black holes. The W02 models have difficulty producing higher mass black holes and so are disfavored. This estimate is affected by the inclusion of Cyg X1 – if Cyg X1 is excluded, the relative probabilities favor the W02 models over the W07 or W07+S14 models by similar factors.

The W07 and W07+S14 cases favor models in which the observed black hole mass function is incomplete at high masses, while the W02 case favors models in which it is incomplete at low masses. This is again a reflection of the relative importance of the two compactness peaks. If we exclude Cyg X1, thereby dropping the (probably) highest mass black hole in the sample, all three models favor a black hole mass function that is incomplete at high masses. These trends are related to the estimate of the black hole formation probability as a function of initial stellar mass by Clausen et al. (2014). Using only the low mass companion systems, their models have a low probability of black hole formation at the compactness peak near $M_0 = 40M_\odot$ that produces the higher mass black holes. This is equivalent to our models

reducing the completeness of the observed sample for higher mass black holes. That our completeness models generally favor incompleteness for high mass systems rather than low mass systems supports the existence of a gap or a deep minimum between the masses of neutrons stars and black holes.

Even with a model allowing large variations in the completeness as a function of mass, we obtain interesting constraints on the compactness leading to black hole formation. We modeled the probability of black hole formation as linearly rising from zero at a minimum compactness $\xi_{2.5}^{min}$ to unity at $\xi_{2.5}^{max}$. The probability of black hole formation should increase monotonically with compactness, but stars of a given mass will really end their lives with a range of compactnesses because of secondary variables other than their initial mass (e.g., composition, rotation, binary interactions). If these secondary variables produce a spread in the compactness at a given initial mass, the finite width of our transition will mimic much of the effect. That being said, the maximum likelihood model was always the one with an abrupt transition ($\xi_{2.5}^{min} = \xi_{2.5}^{max}$), although probability of $\xi_{2.5}^{max} - \xi_{2.5}^{min} > 0$ only declines slowly and the width of the transition is not well constrained. For models in which the completeness is mass-independent, we find $\xi_{2.5}^{min} = 0.15$ ($0.06 < \xi_{2.5}^{min} < 0.20$) and $\xi_{2.5}^{50\%} = 0.23$ ($0.17 < \xi_{2.5}^{50\%} < 0.33$) where $\xi_{2.5}^{50\%} = (\xi_{2.5}^{min} + \xi_{2.5}^{max})/2$ is the compactness at which the black hole formation probability is 50%. Because the width of the transition is poorly constrained, $\xi_{2.5}^{50\%}$ has smaller uncertainties than $\xi_{2.5}^{min}$. If we marginalize over the completeness model, we find $\xi_{2.5}^{min} = 0.18$ ($0.05 < \xi_{2.5}^{min} < 0.23$) and $\xi_{2.5}^{50\%} = 0.24$ ($0.15 < \xi_{2.5}^{50\%} < 0.37$). The upper limits change little, but the lower limits become softer because of the contribution from models with high incompleteness at low black hole mass. These results are for the W07 models, but the results for the other two cases are similar.

The fraction of core collapses predicted to form black holes is relatively high. For the W07 model with no mass-dependent completeness corrections, $f = 0.21$ ($0.11 < f < 0.34$), while after marginalizing over the completeness corrections, $f = 0.18$ ($0.09 < f < 0.39$). The results for the other model sequences are similar. This fraction assumes a Salpeter IMF where all stars from $M_0 = 8M_\odot$ to the maximum mass in the model sequence undergo core collapse. It also assumes that the probability of black hole formation for $\xi_{2.5} > \xi_{2.5}^{max}$ is unity, $P_{max} \equiv 1$. Lowering M_0 or P_{max} would reduce f , while raising M_0 would increase f . For example, raising the minimum mass for core collapse from $8M_\odot$ to $9M_\odot$ raises f by 18%. The probability of black hole formation as a function of initial stellar mass is a complex function reflecting the structure of $\xi_{2.5}(M_0)$. Generically, the probability drops rapidly below $M_0 = 20M_\odot$ in order to minimize the production of low mass black holes and is unity near $M_0 = 20\text{--}25M_\odot$ and $M_0 = 40M_\odot$ where the compactness peaks. At other mass ranges, the probabilities vary greatly with $\xi_{2.5}^{min}$ and $\xi_{2.5}^{max}$.

The most interesting directions for expansion would be to consider other potential indicators of outcomes, such as binding energies, other sequences of stellar models, and other possible definitions of the black hole mass. In particular, many model sequences of ccSN progenitors span only portions of the mass range of interest, frequently with large spacings in mass. In order to carry out the

analysis, this approach requires the full mass range from $M_0 \sim 8M_\odot$ to $M_0 \sim 100M_\odot$. While the differences between the densely sampled Sukhbold & Woosley (2014) and the sparser Woosley & Heger (2007) models in the mass range $15M_\odot < M_0 < 30M_\odot$ seem to have little consequence for our results, we are concerned that the sparse sampling of the Woosley & Heger (2007) models near $M_0 \sim 40M_\odot$ compared to the more densely sampled Woosley et al. (2002) models may drive some differences in the contribution of stars in this mass range to the black hole mass function. Our approach, including models of sample completeness, could also be used to fit sequences of fall-back models (e.g., Zhang et al. 2008, Fryer et al. 2012) to the black hole mass function. We have not done so here because these fall-back models produce continuous mass functions that are completely incompatible with the existing data.

We used a fairly minimalist prior on the fraction of failed ccSNe based on the Galactic ccSN rate and the absence of any neutrino detections of core collapse (Adams et al. 2013). Stronger priors could be developed based on the detections of ccSN progenitors (e.g., Smartt et al. 2009), limits on the rate of failed ccSN (Kochanek et al. 2008, Gerke et al. 2014), the neutron star mass function (Pejcha et al. 2012), the diffuse neutrino background produced by ccSNe (Lien et al. 2010, Lunardini 2009) or comparisons of the star and ccSN rates (Horiuchi et al. 2011, Botticella et al. 2012). The present results are consistent with the available constraints, and roughly predict the mass range and fraction of failed ccSNe needed to explain the red supergiant problem.

ACKNOWLEDGMENTS

We thank T. Sukhbold and S. Woosley for sharing the helium core masses and compactnesses for their expanded set of progenitor models. We thank J.F. Beacom, D. Clausen, A. Gould, C. Ott, T. Piro, K.Z. Stanek and T.A. Thompson for comments and discussions.

REFERENCES

- Adams, S. M., Kochanek, C. S., Beacom, J. F., Vagins, M. R., & Stanek, K. Z. 2013, *ApJ*, 778, 164
- Bailyn, C. D., Jain, R. K., Coppi, P., & Orosz, J. A. 1998, *ApJ*, 499, 367
- Botticella, M. T., Smartt, S. J., Kennicutt, R. C., et al. 2012, *AAP*, 537, A132
- Burrows, A. 1987, *Physics Today*, 40, 28
- Clausen, D., Piro, A. L., & Ott, C. D. 2014, *arXiv:1406.4869*
- Couch, S. M. 2013, *ApJ*, 775, 35
- Couch, S. M., & O'Connor, E. P. 2014, *ApJ*, 785, 123
- Dolence, J. C., Burrows, A., Murphy, J. W., & Nordhaus, J. 2013, *ApJ*, 765, 110
- Dolence, J. C., Burrows, A., & Zhang, W. 2014, *arXiv:1403.6115*
- Farr, W. M., Sravan, N., Cantrell, A., et al. 2011, *ApJ*, 741, 103
- Fryer, C. L., Belczynski, K., Wiktorowicz, G., et al. 2012, *ApJ*, 749, 91

- Gerke, J., et al., 2014, in preparation
- Hanke, F., Marek, A., Müller, B., & Janka, H.-T. 2012, *ApJ*, 755, 138
- Horiuchi, S., Beacom, J. F., Kochanek, C. S., et al. 2011, *ApJ*, 738, 154
- Janka, H.-T., Müller, B., Kitaura, F. S., & Buras, R. 2008, *AAP*, 485, 199
- Kitaura, F. S., Janka, H.-T., & Hillebrandt, W. 2006, *AAP*, 450, 345
- Kiziltan, B., Kottas, A., De Yoreo, M., & Thorsett, S. E. 2013, *ApJ*, 778, 66
- Kochanek, C. S., Beacom, J. F., Kistler, M. D., et al. 2008, *ApJ*, 684, 1336
- Kochanek, C. S. 2014, *ApJ*, 785, 28
- Kreidberg, L., Bailyn, C. D., Farr, W. M., & Kalogera, V. 2012, *ApJ*, 757, 36
- Li, W., Leaman, J., Chornock, R., et al. 2011, *MNRAS*, 412, 1441
- Lien, A., Fields, B. D., & Beacom, J. F. 2010, *PRD*, 81, 083001
- Lovegrove, E., & Woosley, S. E. 2013, *ApJ*, 769, 109
- Lunardini, C. 2009, *Physical Review Letters*, 102, 231101
- Nadezhin, D. K. 1980, *Ap&SS*, 69, 115
- Nordhaus, J., Burrows, A., Almgren, A., & Bell, J. 2010, *ApJ*, 720, 694
- O'Connor, E., & Ott, C. D. 2011, *ApJ*, 730, 70
- Orosz, J. A., McClintock, J. E., Aufdenberg, J. P., et al. 2011, *ApJ*, 742, 84
- Özel, F., Psaltis, D., Narayan, R., & McClintock, J. E. 2010, *ApJ*, 725, 1918
- Özel, F., Psaltis, D., Narayan, R., & Santos Villarreal, A. 2012, *ApJ*, 757, 55
- Pejcha, O., Thompson, T. A., & Kochanek, C. S. 2012, *MNRAS*, 424, 1570
- Smartt, S. J., Eldridge, J. J., Crockett, R. M., & Maund, J. R. 2009, *MNRAS*, 395, 1409
- Sukhbold, T., & Woosley, S. E. 2014, *ApJ*, 783, 10
- Takiwaki, T., Kotake, K., & Suwa, Y. 2012, *ApJ*, 749, 98
- Thompson, T. A., Burrows, A., & Pinto, P. A. 2003, *ApJ*, 592, 434
- Ugliano, M., Janka, H.-T., Marek, A., & Arcones, A. 2012, *ApJ*, 757, 69
- Wong, T.-W., Fryer, C. L., Ellinger, C. I., Rockefeller, G., & Kalogera, V. 2014, arXiv:1401.3032
- Woosley, S. E., Heger, A., & Weaver, T. A. 2002, *Reviews of Modern Physics*, 74, 1015
- Woosley, S. E., & Heger, A. 2007, *Physics Reports*, 442, 269
- Zhang, W., Woosley, S. E., & Heger, A. 2008, *ApJ*, 679, 639
- Ziółkowski, J. 2014, *MNRAS*, 440, L61